Ecological Applications, 24(7), 2014, pp. 1638–1650

Centennial impacts of fragmentation on the canopy structure of tropical montane forest

Nicholas R. Vaughn,[1,2,3] Gregory P. Asner,[1] and Christian P. Giardina[2]

[1]*Department of Global Ecology, Carnegie Institution for Science, Stanford, California 94305 USA*
[2]*Institute for Pacific Islands Forestry, USDA Forest Service, Hilo, Hawai'i 96720 USA*

Abstract. Fragmentation poses one of the greatest threats to tropical forests with short-term changes to the structure of forest canopies affecting microclimate, tree mortality, and growth. Yet the long-term effects of fragmentation are poorly understood because (1) most effects require many decades to materialize, but long-term studies are very rare, (2) the effects of edges on forest canopy structure as a function of fragment size are unknown, and (3) edge effects are often confounded by fragment shape. We quantified the long-term (centennial) effects of fragmentation on forest canopy structure using airborne light detection and ranging (LiDAR) of 1060 Hawaiian rain forest fragments ranging in size from 0.02 to 1000 ha, created more than 130 years ago by flowing lava. Along with distance from edge, we developed a metric, minimum span, to gain additional insight into edge effects on three measures of canopy structure: canopy height, height variation, and gap fraction.

Fragment size was a strong determinant of the three structural variables. Larger fragments had greater average height, larger variation in height, and smaller gap fraction. Minimum span had a large effect on the depth and magnitude of edge effects for the three structural variables. Locations associated with high span values (those surrounded by more forest habitat) showed little effect of distance to fragment edge. In contrast, locations with low span values (those more exposed to edges) were severely limited in canopy height, showed lower height variation, and were associated with greater gap fraction values. The minimum span attribute allows for a more accurate characterization of edge as well as fragment-level effects, and when combined with high resolution imagery, can improve planning of protected areas for long-term ecological sustainability and biodiversity protection.

Key words: *canopy height; Carnegie Airborne Observatory; edge effects; gap fraction; Hawaii; kipuka; LiDAR;* Metrosideros polymorpha; *minimum span.*

Introduction

Forest canopy structure, or the quantity, properties, and spatial arrangement of leaves and branches within the canopy, plays a central role in the functioning of forest ecosystems. Most significantly, canopy structure affects the amount of absorbed solar radiation (Russell et al. 1989) while simultaneously controlling transmitted light available to the forest floor, with understory plants being affected by and also affecting light regime (Montgomery and Chazdon 2001). Variations in canopy density and composition affect seedling survival rates (Kobe 1999, Nicotra et al. 1999) and eventually contribute to variation in understory species composition (Lieberman et al. 1995). The amount of leaf surface area, often measured as leaf area index (LAI), also regulates canopy-scale gas exchange, with effects on stand-level photosynthesis and productivity. Accordingly, LAI controls productivity estimation in some physiological growth models (Running and Gower 1991, Asner et al. 2003, Weiskittel et al. 2011). Through productivity, as well as alteration of temperature and moisture conditions, the canopy also mediates nutrient cycling (Prescott 2002). Species composition of the overstory can also affect nutrient composition of the soil (Binkley and Giardina 1998). As countless forestry studies have shown, changes in nutrient status can subsequently feedback on the status of canopy structure and productivity.

Given the dominant influence of canopies over numerous facets of forest function, disturbances such as fragmentation that affect structure can have cascading effects on most components of an ecosystem. Human-driven fragmentation is a disturbance occurring on a global scale (Riitters et al. 2000), with resulting severe and often large-scale habitat reductions as a two stage process. The first stage is the immediate loss of habitat from the actions that create fragments. The second stage involves the loss of habitat from primary and secondary effects (Harper et al. 2005). Primary effects are physical changes resulting from proximity to newly created edges. These come from an immediate increase in exposure to wind and sunlight, leading to reduced soil moisture, increased desiccation, and increased wind throw of live trees (Matlack 1993, Chen et al. 1995, Kapos et al. 1997). These shifts lead to the

Manuscript received 14 August 2013; revised 10 December 2013; accepted 31 January 2014. Corresponding Editor: C. Sieg.
[3] E-mail: nvaughn@carnegiescience.edu

secondary changes in stand dynamics (Laurance 2002, Pütz et al. 2011), seedling germination rates (Bruna 1999, Benitez-Malvido and Martínez-Ramos 2003), and composition of tree communities (Suzuki et al. 2013). Studies have linked fragmentation or its associated edge transformation to sustained ecosystem decline and changes in species composition (Saunders et al. 1991, Fahrig 2003, Krauss et al. 2010). Biodiversity loss is especially troublesome in tropical regions, which harbor the greatest share of the planet's terrestrial biodiversity (Gardner et al. 2009). To mitigate forest cover loss due to fragmentation, local to regional conservation efforts have attempted to set aside protected areas with the goal to provide suitable habitat for at-risk species (Lindenmayer and Fischer 2006).

An assessment of the suitability of a potential reserve should consider its long-term performance, but little is known about how reserves, sometimes fragments themselves, behave or change over long periods of time. The processes initiated by the creation of a forest edge may take many decades to be realized (Pütz et al. 2011). The effect of a newly created edge on any one tree depends on the combined effects of its neighbors, which in turn are affected by their neighbors. Because plants are long-lived, the plant community may react slowly to their new environments, and through mortality or changes in growth rate, they also alter their effects on neighbors. Additionally, established trees present at the creation of a fragment will be influenced by the effects differently than those that colonize the site afterward. Thus, while changes in individual trees and plants can occur over a relatively short period of time, changes in communities can take many generations to achieve any stable configuration. Critically, the oldest designed fragmentation experiment has not yet reached 35 years of age (Laurance et al. 2011), and few studies present fragments that have persisted without further alteration through a long enough period of time (Corlett and Turner 1997). Thus, there is a major gap in knowledge on how the size of older fragments affects forest structure and function (Ewers and Didham 2006).

Adding further challenge to the study of the long-term fragmentation effects on forests is that the true effects of fragment size are often confounded by the interaction of edge effects and fragment shape complexity (Ewers et al. 2007). Shape complexity is often defined using ratios of area and perimeter or comparing these values to a simple circle. If one assumes a certain depth-of-edge influence, the complex fragment then has less unaffected or core area. This is the main idea behind a commonly used model of edge impacts on fragments (Laurance and Yensen 1991). However, this simple model underpredicts the amount of core area and requires corrections to fit observed and modeled data (Laurance and Yensen 1991, Didham and Ewers 2012). Rather than approach this problem by modeling data with fragment-level effects, another approach is to use only local site characteristics for collected data points. Consideration of the proximity to multiple edges has been shown to increase model fit for edge effects (Fletcher 2005, Harper et al. 2007). A thorough understanding of the complex effects of edge on canopy structure would aid efforts to map how these effects scale up to entire fragments.

We address two questions: (1) how far do fragmentation-initiated alterations to forest canopies extend from the forest edge into the center of fragments more than 130 years after isolation?; and (2) how are within-fragment patterns affected by local fragment shape? To address these questions, we took advantage of a system of naturally fragmented forest islands on the northeast slope of the Mauna Loa volcano on the island of Hawai'i. The native montane tropical forest was fragmented by two landscape-scale lava flow events in 1855 and 1881, and these fragments have been preserved with very little direct human influence for the last 132–158 years (Flaspohler et al. 2010). Using a fine-scale approach made possible with airborne light detection and ranging (LiDAR), we mapped variation in canopy structure within a subsample of the 1060 fragments residing in an area of 8500 ha. By implementing a new metric developed for this study, minimum span, we attempt to disentangle the effects of fragment size and fragment shape. We hypothesized that, after more than a century since isolation, fragmentation effects would continue to permeate up to several hundred meters into the individual fragments, and that the strength of edge effects within the fragments would vary depending on the local edge environment, specifically proximity to nearest and second nearest edges.

Methods

Study site

The study site (19°39′ N, 155°21′ W) is located about 30 km west of the city of Hilo on the island of Hawai'i. Of the island's five volcanoes, the largest is Mauna Loa (4169 m above sea level), an active shield volcano with 33 recorded eruptions since recording began in 1843 (Lockwood and Lipman 1987). Two larger eruptions in 1855 and 1881 produced a large volume of lava along the northeast slope of the volcano. After passing through our study site, the flows left behind nearly one thousand forest fragments, ranging in size from <0.1 to >200 ha, all embedded in a matrix of bare lava rock (Fig. 1). While plants are colonizing the new substrate in the matrix between fragments, primary succession is slow, especially in this high elevation area, and growth rates and heights of sparse individuals are low.

The climate of Hawai'i is tropical, and our study site receives an average of 2400 mm of rainfall annually. However, the montane elevation of the study site, 1400–2000 m, results in cool temperatures. Because of Hawai'i's isolation, the overstory composition is composed of very few species. *Metrosideros polymorpha* (ohia), a common evergreen native tree species in the Hawaiian Islands holds nearly complete dominance. Another native species, *Acacia koa* (koa), occurs in the

canopy with *M. polymorpha*, but in limited numbers (Flaspohler et al. 2010). Understory plant species are relatively uniform across the fragments as well, with key species including *Cheirodendron trigynum* (olapa), *Cibotium glaucum* (hapuu), *Coprosma montana* (pilo), *Ilex anomala* (kawau), and *Myrsine lessertiana* (kolea; Flaspohler et al. 2010). The large number of replications along with uniform vegetation, substrate, and terrain make this an ideal system for the study of fragmentation. Other natural study sites with lava-formed forest fragments do exist (Thébaud and Strasberg 1997), but they are rare and not of the same large scale.

LiDAR data collection

On 10 and 13 January 2008, the Carnegie Airborne Observatory (CAO) Beta system (Asner et al. 2007) was flown over the area at a height of 2500 m above ground level at an average speed of 75 knots (~38.6 m/s). The CAO-Beta LiDAR was a custom-built system with a laser beam divergence of 0.56 mrad and a laser wavelength of 1064 nm. For this data collection, the LiDAR pulse frequency was set to 33 kHz, scan frequency to 10 Hz, and half-scan angle set at 17 degrees. Swath overlap was nominally 35–40%. Up to four discrete returns per pulse were recorded. These flight and instrument settings yielded a data set of 1.17 returns per m^2, on average, over the vegetated areas. Using this system, prior work has found that errors in positioning at the sensor have a standard deviation of 7 cm vertical and 5 cm horizontal.

Mapping canopy height and structure

The heights of the LiDAR returns above the ground are of particular interest when assessing vegetation structure. A common first step is then to create a model of ground elevation for our study area, typically referred to as a digital elevation model (DEM), from the LiDAR data set. The process starts with identifying the LiDAR returns that correspond to ground surface locations. The ground elevation is then interpolated between these points, using one of many methods, to create a raster file containing ground elevations on a regular grid representing the area of interest. Using the las2dem program, which is part of the LASTools suite (Isenburg 2013), a 2 × 2 m DEM was created for this project, covering 9012 × 9506 m.

Statistics describing the distributions of return heights are simple, yet very informative descriptors of canopy structure. At the center of each 2 × 2 m DEM grid cell center, we collected all LiDAR returns falling within a square 18 × 18 m window centered at the same point as the cell center. This means that the windows for adjacent 2 × 2 m cells overlap by 89 %, and the two cells therefore have a large number of window returns in common. Larger windows would have values with much more stability, but smaller windows can better capture the changes that are visible over short distances from fragment edges. After testing several window sizes, 18 m was chosen as the value that best met both restrictions.

Within each 18 m window, we sorted these neighborhood returns by height above their respective DEM cells. To remove the influence of large numbers of ground and low vegetation points from the analyses, we discarded returns less than 1.5 m above ground. This value was chosen as the upper tail of the first peak in a histogram of the height above ground of all returns. From the remaining ordered returns, we computed both the maximum height (HT) as well as the difference in height between the 75th percentile and the 25th percentile (IQR). IQR provides a quantification of the vertical dispersion of the LiDAR returns, which is strongly correlated with canopy depth. Both HT and IQR for each cell center were then recorded into a raster image file for quick look up and reference.

As an index for the capacity of a canopy to absorb photosynthetically active radiation, we estimated gap fraction (GF) at all cell centers in the same 2 × 2 m grid across the study area. LAI estimates from specialized instruments are biased in this forest type (Herbert and Fownes 1997) because of the high leaf aggregation in *M. polymorpha*. Because *M. polymorpha* is so dominant in this region and the canopy species are then uniform across the landscape, GF should be a robust indicator of the interception potential of the canopy. GF was estimated from the LiDAR data using the polar grid fraction metric (Vaughn et al. 2013). Briefly, polar grid fraction is calculated by dividing the upward hemispherical view from a given point into wedges that are defined by intervals of zenith and azimuth angles. For our study, azimuth angle was divided evenly into sixteen intervals, and zenith angle was divided into 24 intervals bounded by uniform steps (0.0175 units wide) in cosine-transformed zenith angle. Polar grid fraction is the proportion of these wedges that contain one or more LiDAR return x,y,z locations. The idea behind the metric is that LiDAR returns represent a known location of vegetation cover, and a variable portion of light would pass through this vegetation to influence gap fraction estimates from a field instrument placed at a given point.

Fragment boundaries

We defined boundaries of fragments using a combination of two raster data sets: the map of LiDAR-derived canopy height and a map of the normalized difference vegetation index (NDVI). The NDVI map was derived from the imaging spectrometer aboard the CAO aircraft (Asner et al. 2007), collected simultaneously with the LiDAR data. To speed the computation in following steps, we interpolated the NDVI data set to the same 2-m grid used in structure analysis. To smooth the rapid changes in the height and NDVI images that can occur at the location of individual trees, we first applied a mean filter (where each cell is changed to the mean of the surrounding cells) to both data sets with a square kernel of size 5 × 5 cells (10 × 10 m) for the canopy height data

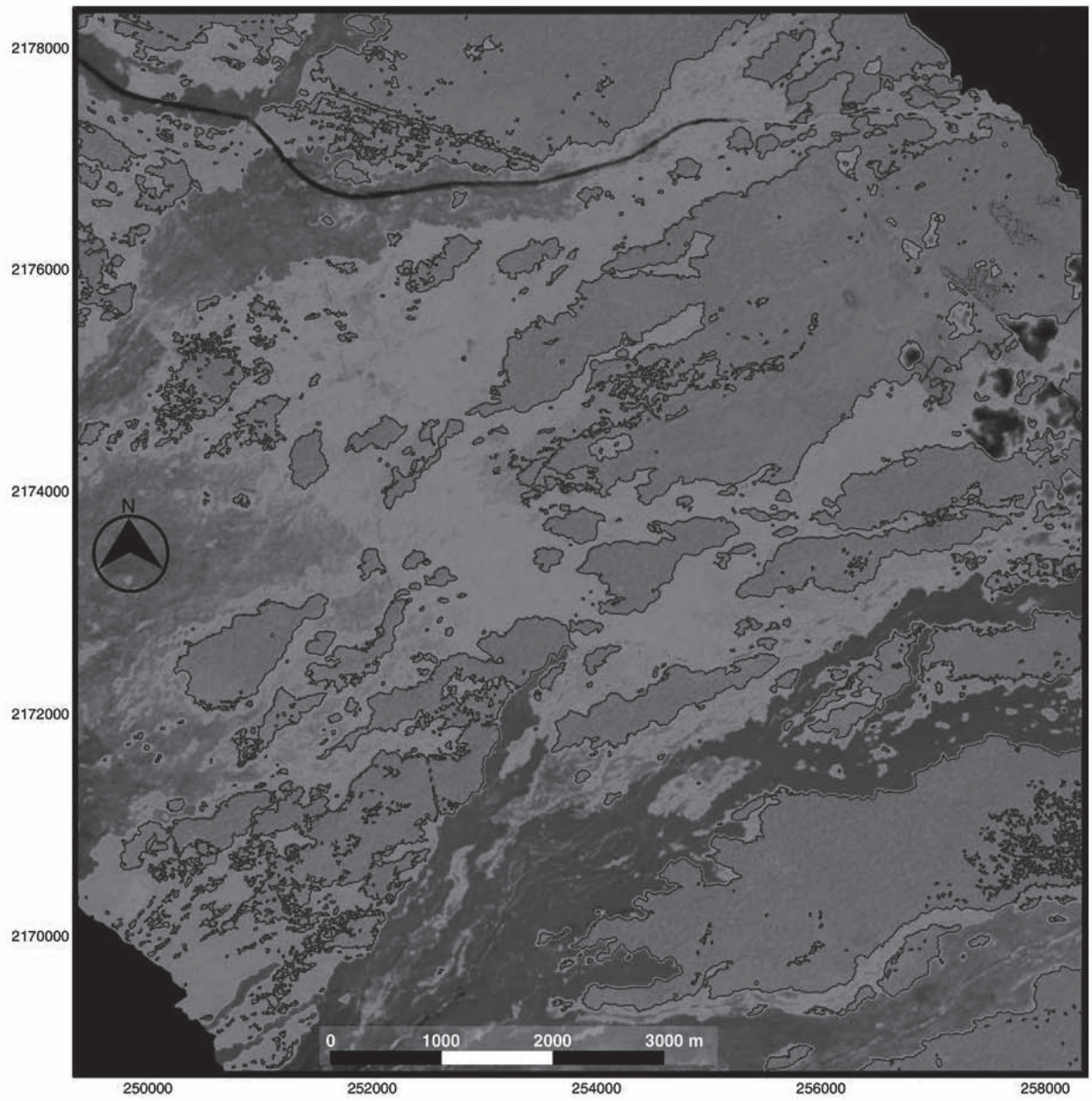

FIG. 1. A map of the 8500-ha study site on the northeastern flank of Mauna Loa volcano, Hawai'i Island. Outlines of the fragments are shown in blue. A normalized difference vegetation index (NDVI) image in the background increasing from brown to green indicates the amount of photosynthetic vegetation present. Recent lava flows from the southwest are visible as darker brown colors, and State Highway 200 can be seen as the dark line from the northwest.

set and 15 × 15 cells (30 × 30 m) for the NDVI data set. We marked all cells with values exceeding two thresholds: 3 m for canopy height and an NDVI value of 0.7, as part of a fragment. We settled on these threshold values because they best defined obvious fragment boundaries and ignored the patches of stunted, sparse ingrowth that has established on the bare rock. However, even considerable changes in these values had little effect on the majority of fragment edges, those that are clearly defined. Clusters of marked cells with fewer than 50 member cells (0.02 ha) were discarded. We then recorded the outline of each remaining cluster as a polygon into a standard geospatial data format for all future analysis (Appendix 1). Because structural variables for matrix habitat were not of interest, all cells in the grids for each canopy structure variable (HT, IQR, and GF) with center falling outside a fragment boundary were set to a null value. Following this, histograms were computed for the three canopy structure variables for all cells within a fragment (Fig. 2).

Fragment size and shape effects

Following the fragment boundary creation procedure, we identified 1060 fragments greater than the 0.02-ha

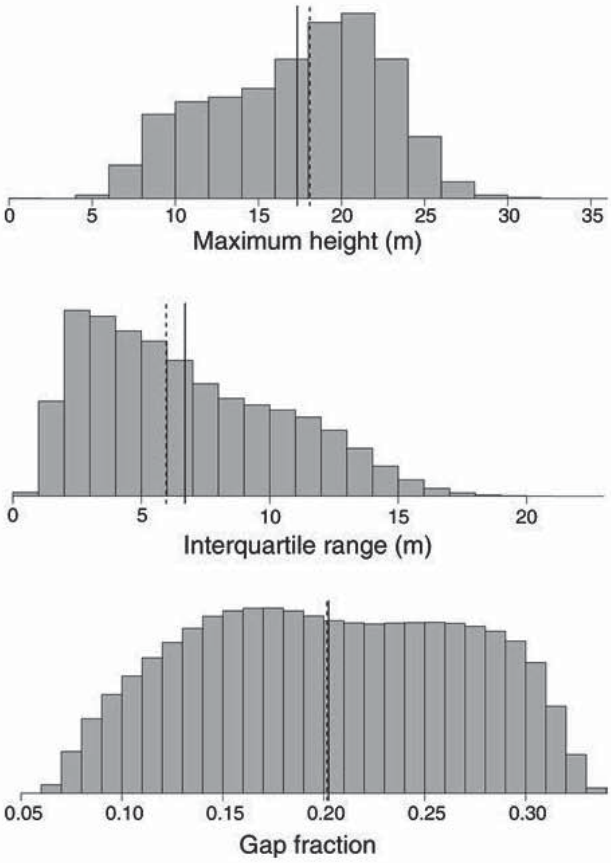

FIG. 2. Histograms of the three canopy structure metrics mapped across the study landscape on Mauna Loa volcano, Hawai'i Island. All 2×2 m cells were used in the computation of these histograms. Solid and dashed vertical lines represent the mean and median, respectively.

threshold for further analyses. The majority of these are less than 1 ha in size, but several fragments exceed 100 ha, with one fragment being nearly 1000 ha (Fig. 3). Fragment size has been implicated before as a driver of differences between fragments at this site (Flaspohler et al. 2010). We investigated the impact of fragment size, along with those of structural metrics using scatterplots and linear regression models of the whole-fragment average canopy metric values against log-transformed fragment size.

Proximity to the fragment edge is commonly considered an important measurable factor affecting the response of a given location to fragmentation (Harper et al. 2005). Preliminary analysis showed that this was indeed the case at our study site. For final analysis, we then computed the distance from nearest fragment edge (DE) at the center of each 2-m cell that was located within a fragment boundary polygon. Because two points with similar DE can differ widely with respect to proximity to a second edge, with implications for habitat quality, we derived a simple metric, minimum span (MS), which is the minimum straight line distance, allowing azimuth to vary 180 degrees, that is required to bisect the fragment while passing through a given point location (Fig. 4a). This metric is essentially a quantification of the protection afforded to a given point by the surrounding fragment, and it can be calculated for any given point within a fragment (Fig. 4b; Supplement 2). Accordingly, MS was computed at the center of every 2-m cell located within each fragment boundary polygon. In this application, azimuth was incremented from 0 to 177 degrees in 3-degree steps to compute minimum span.

Due to the high correlation between neighboring cells and the extremely large number of cells, we randomly selected a subset of 10 000 2×2 m cells containing valid values for both of the covariates DE and MS, as well as valid values for all three response variables of HT, IQR, and GF. These samples were contained by 268 of the original 1060 identified fragments. Initially, we produced boxplots from these data to visually assess the effects of the two covariates, DE and MS on the three canopy structure variables. The main effects were cut into fixed intervals to inspect for any interaction. MS was cut into five intervals: (0,20], (20,50], (50, 100], (100, 200] and >200, while DE was cut into six intervals: (0,5], (5,10], (10,20], (20,50], (50, 100], and >100. For each possible combination (DE must be less than half of the MS for a given location) a box plot was created with the 5th, 10th, 25th, 50th, 75th, 90th, and 95th percentiles.

The relationship between the two covariates and the response variables was curvilinear in all cases in such a way that the slope of the response curve decreases as the covariates increase in value. Initially, simple linear models were run with both covariates, MS, and DE, as well as an interaction term, but this did not sufficiently fit the data. To more accurately model the curvilinear pattern, both covariates were log-transformed before

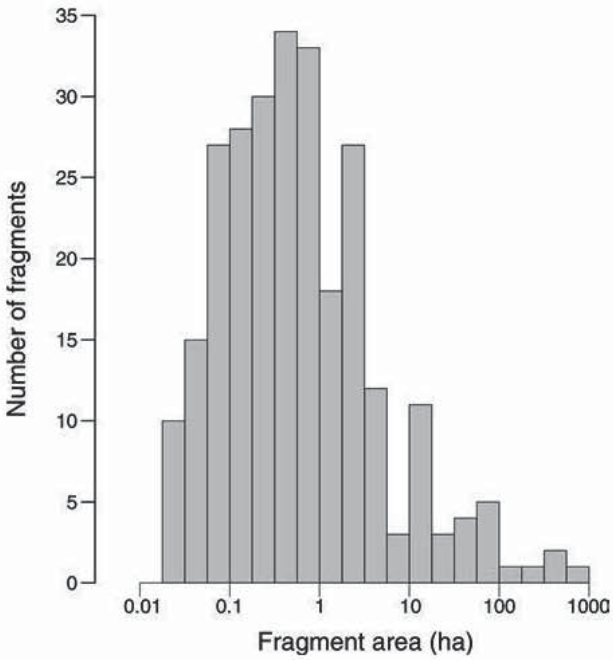

FIG. 3. A histogram of the sizes of the 268 forest fragments with sample points across the study landscape on Mauna Loa volcano, Hawai'i Island. Note the log scale on the *x*-axis.

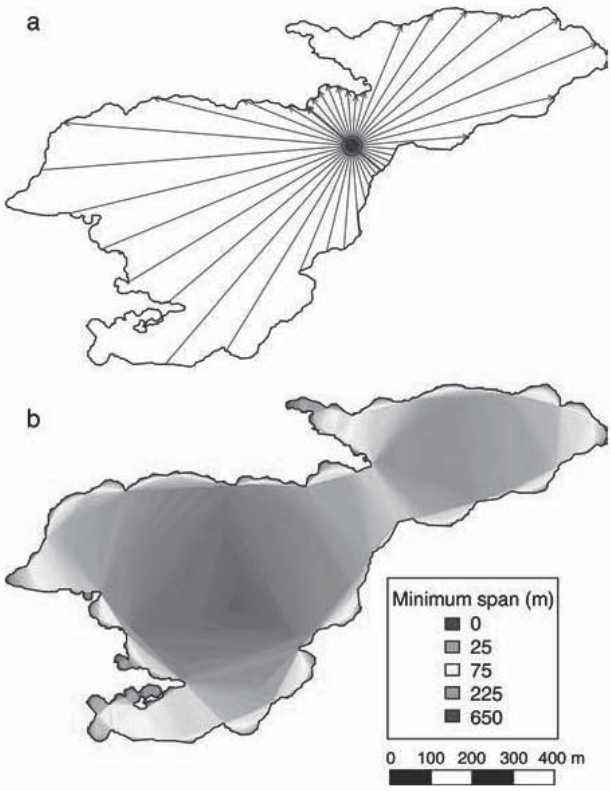

FIG. 4. A demonstration of the minimum span concept with data from across the study landscape on Mauna Loa volcano, Hawai'i Island. (a) For the given point at the center of red circles, the span can be computed in any direction as the straight-line distance required to strike two locations along the fragment boundary as well as the point. Many such spans are shown as black arrows. The minimum span (MS) is the shortest across all angles (red arrow). (b) Minimum span mapped on a 2 × 2 m grid for a larger, complex-shaped fragment.

being included in the model. The increasing variance (decreasing for GF) that is visible in the box plots was addressed by log-transforming each of the three response variables, HT, IQR, and 1 − GF (negated so that variance would increase with mean). We fit one model for each of the three structural response variables. In such a way, the individual and combined influence of DE and MS could be interpreted.

The residuals from simple linear fit of the three models showed significant spatial autocovariance, as determined by a Moran's I test (Table 1). This introduces the potential for biased estimates of both the fitted coefficients and their standard errors. To overcome this, we used a spatial autoregressive (SAR) modeling framework to account for stationary, isotropic correlation among residuals. These fits were computed using the R programming language (R Development Core Team 2012), incorporating the spdep contributed package (Bivand 2012). Neighbors within 200 m, a distance determined from inspection of correlograms, were included in the computation of the weight matrix.

RESULTS

Strong effects of fragmentation were found in all three structural variables that were tested. Fragment size explained more than one-third of the variation among fragment mean GF values, but the same model had lower goodness of fit for both HT and IQR (Fig. 5). As fragment size increased, expected HT increased from 10 to ~20 m and expected IQR increased from 2 to 8 m, indicating that larger fragments are associated with greater variation in tree size. We also found that GF decreased from 0.3 for smaller fragments to about 0.15 for the largest fragments. In addition to fragment-level variation, we observed large intrafragment spatial variation among the different DE and MS interval combinations for all three response variables (Fig. 6).

Interpreting DE and MS as continuous variables in a linear model improved our ability to understand the relative strength of the two variables as well as their interaction. Three important features of this model parameterization should be noted. First, the model estimates will depend upon DE only up to a certain distance (although never more than one half of the minimum span) and upon MS only up to a certain distance. In this way, the interiors of fragments behave more like intact forest than at the edges, and the marginal effect of each covariate will diminish. Second, a significant slope for log(MS) means that the maximum value of the response variable will change with MS, independent of the value of DE. A third and very important feature is that significant model interaction terms indicate that the rate at which the response value climbs to its maximum with respect to DE also changes as MS increases. This allows for a shrinking depth of noticeable edge effect as MS increases, or nonuniform edge effects.

Using the spatial error SAR modeling methodology reduced the autocovariance present in the residuals

TABLE 1. Moran's I tests of the spatial autocorrelation of the residuals for the three models with a simple least squares regression (OLS) model (top rows) and with a spatial error (SAR) model (bottom rows).

Response	Model	Moran's I	Var(I)	Statistic	P
log(HT)	OLS	0.591	8.906×10^{-6}	198.13	<0.00001
log(IQR)	OLS	0.511	8.907×10^{-6}	171.20	<0.00001
log(1 − GF)	OLS	0.545	8.908×10^{-6}	182.76	<0.00001
log(HT)	SAR	−0.007	8.905×10^{-6}	−2.23	0.98701
log(IQR)	SAR	−0.011	8.906×10^{-6}	−3.75	0.99991
log(1 − GF)	SAR	−0.015	8.907×10^{-6}	−4.86	1.00000

Note: The expected value of I was -1.001×10^{-4} in all cases.

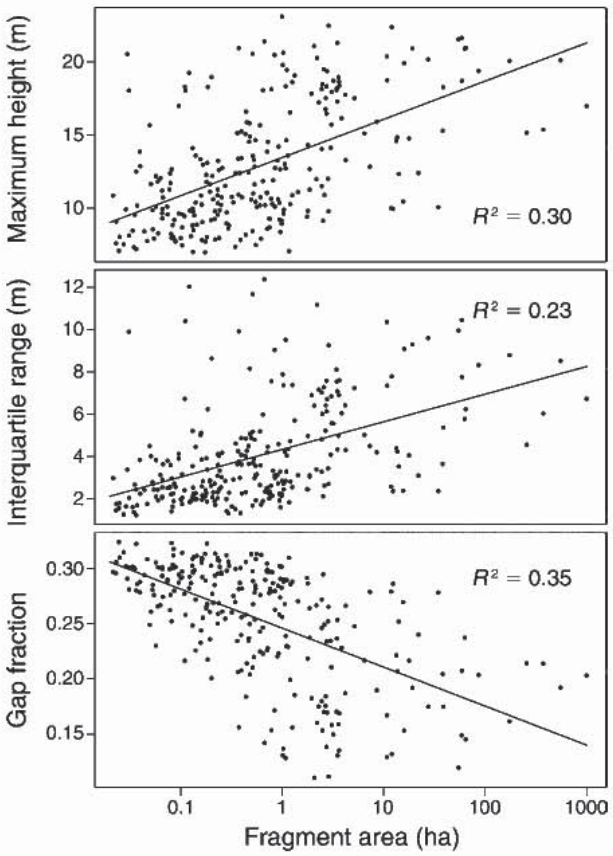

FIG. 5. Scatterplots of the three canopy structural variables against fragment size for data sampled across the study landscape on Mauna Loa volcano, Hawai'i Island. Best-fit lines along with the associated R^2 values are shown. Points represent the mean value of a structural variable, across all 2 × 2 m cells within the fragment or the total area for a single fragment.

(Table 1). Residuals from these models produced Moran's I statistics very near to the expected value under the null hypothesis of no autocovariance present. The resulting linear coefficients of log(DE) and log(MS) were very close in scale (Table 2). Interaction terms were highly significant except in the regression for IQR. Signs of the coefficient on the interaction variable were opposite those of the main effects in each case, which, in effect, allows estimated response value to increase more and more slowly as DE and MS get larger. Under these realized models, estimates of each structural variable, along with their expected ranges, then progress towards asymptotic values as the estimators reach large values (Figs. 7 and 8). The larger the MS value, the faster this progression takes place, with the largest values of MS strongly reducing the effect of DE even at the edges.

Discussion

Our results provide compelling evidence for persistent, centennial-scale changes in canopy structure following forest fragmentation, with the strongest impacts occurring at fragment edges for all three properties of forest canopy structure. We found that these edge differences were expressed at the whole-fragment level as well: larger fragments, characterized by lower edge to core habitat, were less affected by the matrix environment overall. Little prior work has demonstrated such long-term effects of fragmentation because it is difficult to find a complete history for fragments that are maintained for longer periods of time (Corlett and Turner 1997). Without accounting for a history of human activities in the area, one cannot fully attribute the observed results to fragmentation alone (McGarigal and Cushman 2002). Designed experiments, which have more control over fragment history, are not yet sufficiently long-lived to study such long-term effects. The natural fragment system used in this study shows uniformity across many factors, including slope, elevation, forest type, soil substrate age, method of fragment creation, fragment age, and matrix condition, with which even designed experiments have difficulty maintaining. Additionally, the site's relative seclusion and designation as a State of Hawaii Forest Reserve have kept human activity in the area to a minimum. Taken together, these traits make this study site ideal for providing insights into the long-term effects of forest fragmentation.

As expected, distance to edge was a strong determinant of forest canopy condition. We found that the expected maximum height to which trees can reach at fragment edges was shorter than interior locations by as much as 7 m. Canopy complexity, as measured by IQR, was also substantially lower near the edges of the fragments. This shorter and more uniform canopy found at the edges of all fragments and the interior of smaller fragments is similar to that of a younger forest. Pütz et al. (2011) found similar state shifts in Brazilian tropical forest fragments. Edge forests face some challenges in the long term due to increased exposure to the surroundings outside of fragments. An increase in wind and solar radiation exposure leads to greater wind throw (Chen et al.1995) and greater loss of moisture (Briant et al. 2010). Accordingly, these differences can drive increased mortality and turnover rates (Laurance et al. 2002). Edge trees that survive the increased exposure are likely limited in maximum achievable height and vertical growth rate, affecting the long-term dynamics of the forest. This would lead to the shorter, more uniform canopy observed in this study.

Another effect of edge creation may be a long-term reduction in forest productivity. Gap fraction has a strong functional link to many processes that control the growth of plants (Campbell and Norman 1989). The estimated gap fraction at edges and within the interior of smaller fragments was significantly smaller. Gap fraction differences were larger than 0.10 in some cases, nearly one-third of the maximum estimated gap fraction value in the study area. In contrast, some early increases in productivity have been found at the edges of younger

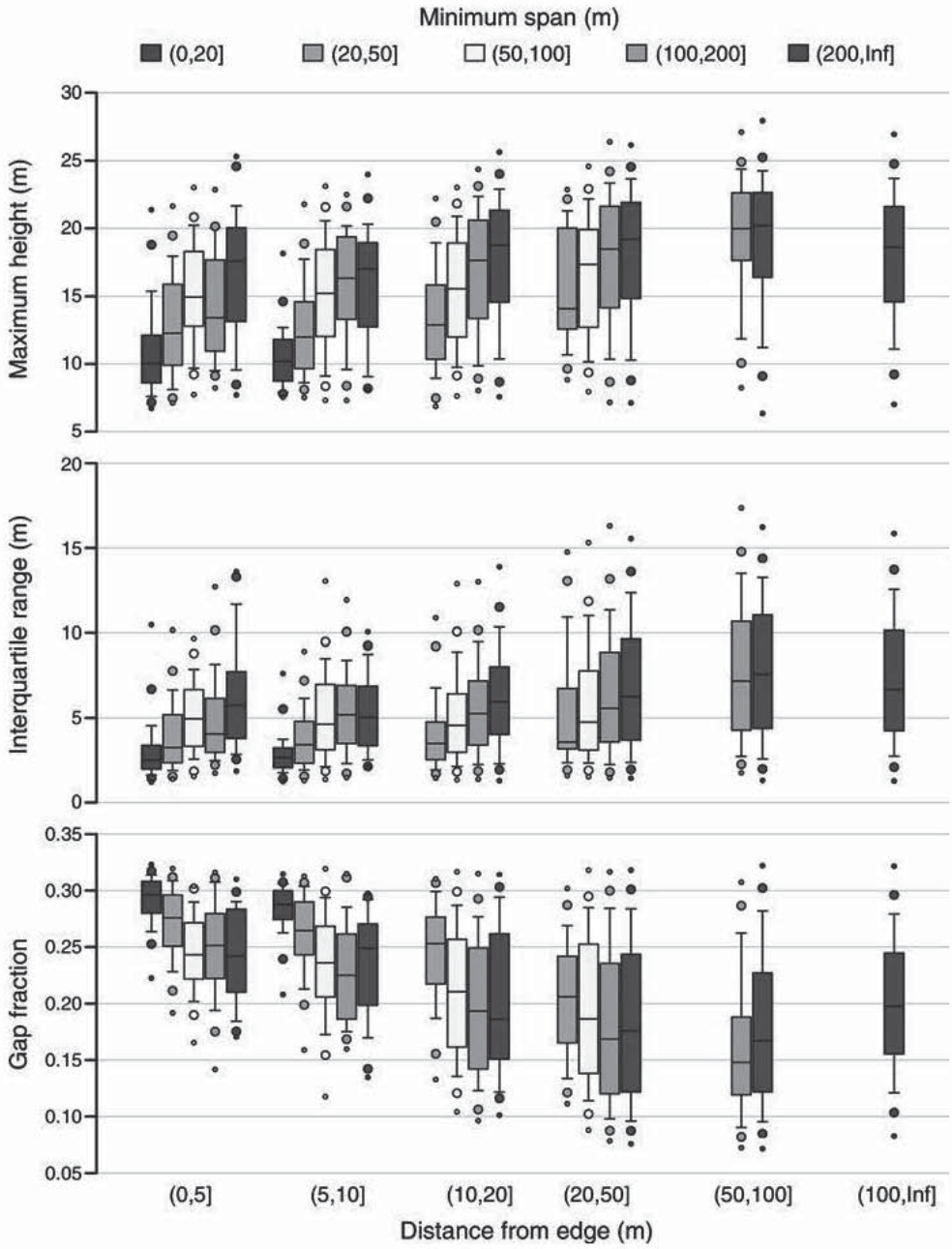

FIG. 6. Boxplots of canopy structure response variable distributions along distance from edge and selected minimum span values from fragments sampled across the study landscape on Mauna Loa volcano, Hawai'i Island. Large dots represent the 5th and 95th percentiles, and small dots represent the 1st and 99th percentiles. The line inside the box is the median. Upper and lower end points are the 75th and 25th percentiles, respectively. Whiskers are the 10th and 90th percentiles. Inf is positive infinity.

fragments (Murcia 1995, Harper et al. 2005). Early increases in productivity can be explained by a large increase in some resources when edge inhabitants find themselves suddenly without competition on one side and young trees colonizing may grow more quickly than the older trees they replace. Light, water, and nutrients all have the potential to be much more abundant at edges (Matlack 1993). However, most edges in the tropics are created by slash and burn methods, with potentially large effects on nutrient supply (Giardina et al. 2000). At our Hawaiian site, the lava flow would have similarly affected edge habitat along with organic material at the surface, albeit with likely different burn effects. Fresh lava rock is also a poor substrate from which to obtain nutrients and water. It is possible that an early increase in productivity took place when these fragments were formed. However, in the long-term, it appears that the effects of a harsher environment have become dominant.

The strength and depth of edge effects on canopy structure within a fragment are highly variable, and a large share of this variability can be explained by the

TABLE 2. List of parameters fit using a spatial autoregressive model (SAR) for each response variable.

Response	Term	Coefficient	SE	Z	P
log(HT)	(Intercept)	2.222	0.0280	79.47	<0.00001
	log(DE)	0.075	0.0077	9.78	<0.00001
	log(MS)	0.073	0.0054	13.63	<0.00001
	log(DE) : log(MS)	−0.007	0.0014	−4.83	<0.00001
log(IQR)	(Intercept)	0.865	0.0524	16.51	<0.00001
	log(DE)	0.069	0.0160	4.30	0.00002
	log(MS)	0.099	0.0114	8.71	<0.00001
	log(DE) : log(MS)	−0.001	0.0029	−0.46	0.64289
log(1 − GF)	(Intercept)	−0.400	0.0069	−58.01	<0.00001
	log(DE)	0.033	0.0020	16.25	<0.00001
	log(MS)	0.021	0.0014	14.68	<0.00001
	log(DE) : log(MS)	−0.003	0.0004	−9.15	<0.00001

Notes: Abbreviations in the Term column correspond to the two covariates: DE is distance from edge, and MS is minimum span. Response variable abbreviations are: HT, maximum window return height; IQR, window interquartile range of return heights; GF, gap fraction.

local shape of a fragment, as quantified by minimum span. For a single point, exposure to the impacts of the foreign matrix habitat does not occur from only one angle, but rather from any direction where an edge falls within some threshold distance. Proximity to multiple edges then should combine to increase or decrease any particular edge effect (Fletcher 2005, Harper et al. 2007). Conversely, when the minimum span for a given point location within a fragment is large enough (as little as 300 m for maximum canopy height), the effect of the distance to edge was reduced dramatically for all three structural response variables. The canopy at a location with small distance-to-edge and large minimum span, despite being exposed to the surrounding matrix on one side, has a larger expected maximum canopy height and a lower gap fraction than sites with low minimum span. This contradicts the uniform edge model suggested by Laurance and Yensen (1991), which is often assumed to be the link between fragment size and fragment shape effects (Ewers and Didham 2007). Such variation in canopy structure among edges within a single fragment indicates that care must be taken in choosing sample locations for studying edge effects. The local variations in edge effects due to shape are large enough in this study to obscure DE effects, if variation due to MS is ignored. While there are several reasons for differences in sign, magnitude, and penetration distance of measured edge effects across studies, perhaps the effects of local fragment shape is an underlying driver.

Our results have implications for the design conservation reserves. The distribution of fragment sizes in our study site is similar to observed size distributions in both the Brazilian Atlantic Forest (Ribeiro et al. 2009) and Amazon rain forest (Broadbent et al. 2008), in that a majority of the fragments are small in area (<50 ha). Change analysis also indicates that fragment sizes are being reduced (Broadbent et al. 2008). Since conservation reserves often draw from remaining, intact forest, there is usually interest in optimizing their functionality as affected by reserve size and shape. It has been observed for decades that size should be an important factor in reserve selection (Higgs and Usher 1980), and this is confirmed by the relationship observed between fragment size and bird species diversity present in these same fragments (Flaspohler et al. 2010). However, size alone is not entirely informative, as fragment shape exerted a large influence on stand characteristics. The interaction between a species and the shape of a reserve may amplify or diminish a species' survival (Ewers and Didham 2007, Harper et al. 2007). One must then somehow account for fragment shape when performing any analysis of the effects of fragmentation.

To account for the effect of shape on the core area that is typically of most benefit in reserves, numerous shape metrics have been developed (Baskent and Jordan 1995, Riitters et al. 1995). Metrics such as diversity index (Patton 1975) and fractal dimension (Milne 1988) that incorporate only fragment perimeter and area imply that edge effects can be modeled as uniform. However, the results presented here indicate that more complex patterns exist, and these need be taken into account when estimating the total suitability of a potential reserve. For tree species, at least, minimum span provides a possible mechanistic explanation for the behavior of differently shaped fragments. Other shape metrics, such as divergence (Baskent and Jordan 1995), incorporate more of the spatial information available from a fragment perimeter. Such metrics may be able to better account for the dynamic relationship seen here between distance to edge and minimum span and might perform better when used to model fragment-level effects.

It is also possible that minimum span statistics may function as a shape metric. Minimum span itself is intended to be more informative at scales smaller than whole fragment and is not meant to be a replacement for the above shape metrics. However, a simple average of the minimum span (or log-transformed minimum span) values across the entire fragment could function as a shape metric. Then to maximize reserve effectiveness, a

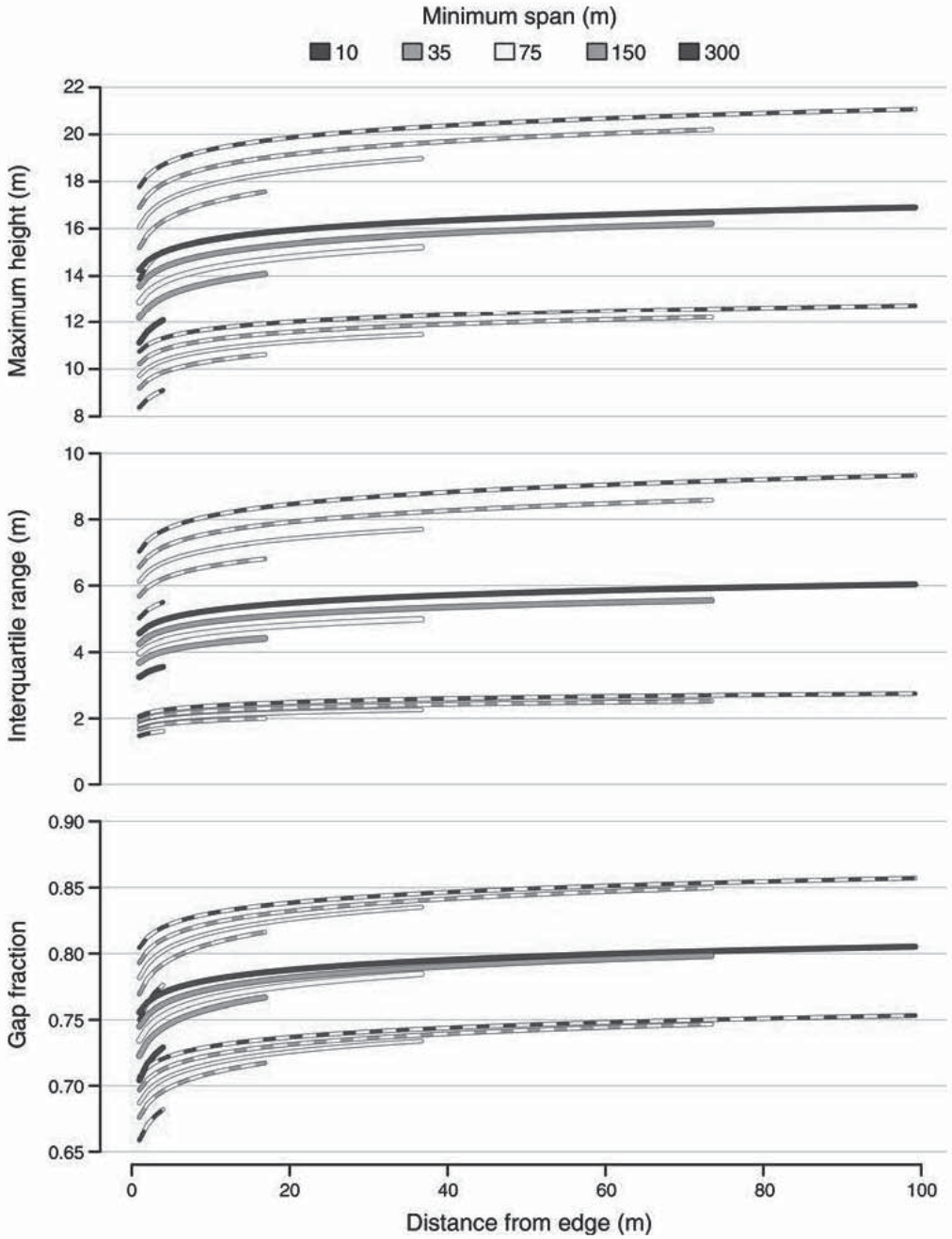

FIG. 7. Estimated median (solid) and 10th and 90th percentiles (dashed) of response variable distributions along distance-to-edge for selected minimum span values for points within fragments sampled across the study landscape on Mauna Loa volcano, Hawai'i Island.

reasonable goal would be to maximize the average minimum span for a given reserve, thus minimizing the overall or average edge effects. The optimal shape under this arrangement would be that which minimized the integrated effects of edge within a fragment. Much like the optima of many shape complexity metrics, the maximum value for minimum span for a given area is attained with a circular shape. Circular reserves also provide the highest core-to-edge-area ratio, and they reduce traversal distance for core-dwelling species (Diamond 1975). Indeed, fewer species are found in peninsula habitat than in core habitat (Blouin and Conner 1985), and this may be due to the effects of minimum span on forest attributes. However, more variation in edge type may be helpful for some species, meaning more complex shapes would provide more variation in habitat types. Despite the differences in edge effect brought on by minimum span, the greatest contributor to increasing minimum span and core-to-edge ratio is simply reserve size.

Finally, we emphasize the importance of the airborne LiDAR data in this study. We quantified the effects of

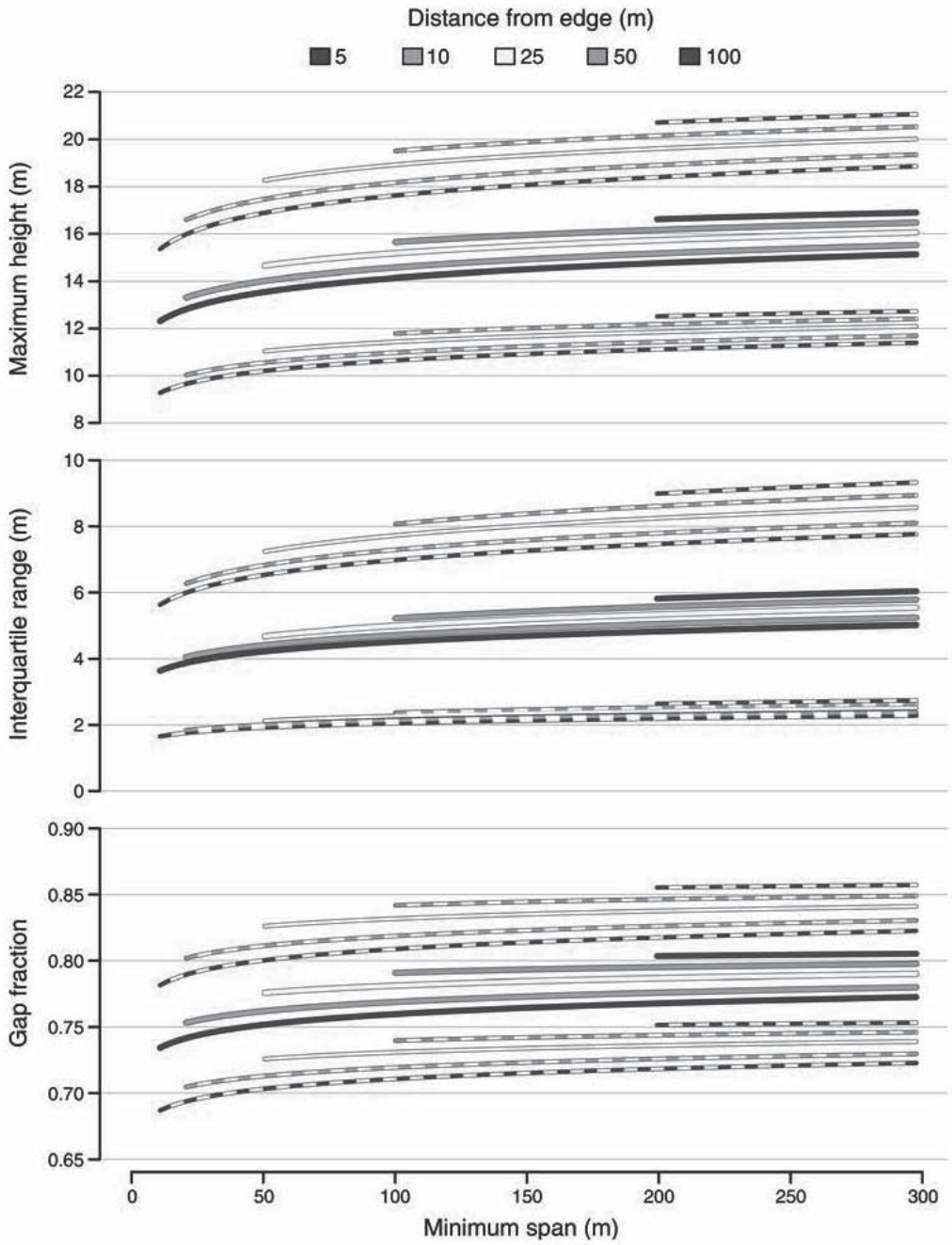

FIG. 8. Estimated median (solid) and 10th and 90th percentiles (dashed) of response variable distributions along minimum span for selected values of distance-to-edge for points within fragments sampled across the study landscape on Mauna Loa volcano, Hawai'i Island.

minimum span and distance to edge across a very large landscape containing myriad fragment shapes and sizes. This work was performed with information organized at a spatial scale ordinarily reserved for the study of microsites. Such work across spatial scales has only been possible for a relatively short time (Chave 2013). With even a small selection of the large number of fragments in the system, understanding the role of local shape on edge effects from field samples would be prohibitively expensive. At another extreme, satellite imagery would give adequate coverage, but not the high spatial resolution needed for this task. Aerial photography would provide the resolution, but limited three-dimensional structure information. Clearly LiDAR methods hold great potential for understanding fragmentation effects on forest structure and function.

ACKNOWLEDGMENTS

This study was supported by the John D. and Catherine T. MacArthur Foundation, the endowment of the Carnegie Institution for Science, National Science Foundation grant

DEB–0715593 (G. P. Asner), and the USDA Forest Service Pacific Southwest Research Station, as well as support from National Science Foundation grants DEB–1020412 (T. Fukami, C. P. Giardina, G. P. Asner), DEB– 1020007 (D. S. Gruner), and DEB–1019928 (D. J. Flaspohler). We thank T. Kennedy-Bowdoin, other Carnegie Airborne Observatory staff members, and D. Leopold for assistance with airborne LiDAR data collection, processing, and analysis. For support of gap fraction estimation, we thank B. Hwang, T. Kovach, C. Phifer, and B. Sung for field measurements, the University of Hawaii at Hilo for access to GPS equipment, and the State of Hawaii Division of Forestry and Wildlife for access to field sites. The Carnegie Airborne Observatory is made possible by the Avatar Alliance Foundation, Grantham Foundation for the Protection of the Environment, John D. and Catherine T. MacArthur Foundation, Gordon and Betty Moore Foundation, W. M. Keck Foundation, Margaret A. Cargill Foundation, Mary Anne Nyburg Baker and G. Leonard Baker, Jr., and William R. Hearst III.

Literature Cited

Asner, G. P., D. E. Knapp, T. Kennedy-Bowdoin, M. O. Jones, R. E. Martin, J. Boardman, and C. B. Field. 2007. Carnegie Airborne Observatory: in-flight fusion of hyperspectral imaging and waveform light detection and ranging for three-dimensional studies of ecosystems. Journal of Applied Remote Sensing 1:013536.

Asner, G. P., J. M. O. Scurlock, and J. A. Hicke. 2003. Global synthesis of leaf area index observations: implications for ecological and remote sensing studies. Global Ecology and Biogeography 12:191–205.

Baskent, E. Z., and G. A. Jordan. 1995. Characterizing spatial structure of forest landscapes. Canadian Journal of Forest Research 25:1830–1849.

Benitez-Malvido, J., and M. Martínez-Ramos. 2003. Influence of edge exposure on tree seedling species recruitment in tropical rain forest fragments. Biotropica 35:530–541.

Binkley, D., and C. P. Giardina. 1998. Why do tree species affect soils? The warp and woof of tree–soil interactions. Biogeochemistry 42:89–106.

Bivand, R. 2012. spdep: spatial dependence: weighting schemes, statistics and models. Version 0.5-45. http://cran.r-project.org

Blouin, M. S., and E. F. Conner. 1985. Is there a best shape for nature reserves? Biological Conservation 32:277–288.

Briant, G., V. Gond, and S. G. W. Laurance. 2010. Habitat fragmentation and the desiccation of forest canopies: a case study from eastern Amazonia. Biological Conservation 143:2763–2769.

Broadbent, E., G. P. Asner, M. Keller, D. E. Knapp, P. Oliveira, and J. N. M. Silva. 2008. Forest fragmentation and edge effects from deforestation and selective logging in the Brazilian Amazon. Biological Conservation 141:1745–1757.

Bruna, E. M. 1999. Biodiversity: seed germination in rainforest fragments. Nature 402:139.

Campbell, R. G., and J. M. Norman. 1989. The description and measurement of plant canopy structure. Pages 1–19 *in* G. Russel, B. Marshall, and P. G. Jarvis, editors. Plant canopies: their growth, form, and function. First edition. Cambridge University Press, Cambridge, UK.

Chave, J. 2013. The problem of pattern and scale in ecology: what have we learned in 20 years? Ecology Letters 16:4–16.

Chen, J., J. F. Franklin, and T. A. Spies. 1995. Growing-season microclimatic gradients from clearcut edges into old-growth Douglas-fir forests. Ecological Applications 5:74–86.

Corlett, R. T., and I. M. Turner. 1997. Long-term survival in tropical forest remnants in Singapore and Hong Kong. Pages 333–345 *in* W. F. Laurance and R. O. Bierregaard, Jr., editors. Tropical forest remnants: ecology, management and conservation of fragmented communities. University of Chicago Press, Chicago, Illinois, USA.

Diamond, J. M. 1975. The island dilemma: lessons of modern biogeographic studies for the design of natural reserves. Biological Conservation 7:129–146.

Didham, R. K., and R. M. Ewers. 2012. Predicting the impacts of edge effects in fragmented habitats: Laurance and Yensen's core area model revisited. Biological Conservation 155:104–110.

Ewers, R. M., and R. K. Didham. 2006. Confounding factors in the detection of species responses to habitat fragmentation. Biological Reviews of the Cambridge Philosophical Society 81:117–142.

Ewers, R. M., and R. K. Didham. 2007. The effect of fragment shape and species' sensitivity to habitat edges on animal population size. Conservation Biology 21:926–936.

Ewers, R. M., S. Thorpe, and R. K. Didham. 2007. Synergistic interactions between edge and area effects in a heavily fragmented landscape. Ecology 88:96–106.

Fahrig, L. 2003. Effects of habitat fragmentation on biodiversity. Annual Review of Ecology, Evolution, and Systematics 34:487–515.

Flaspohler, D. J., C. P. Giardina, G. P. Asner, P. Hart, J. Price, C. K. Lyons, and X. Castaneda. 2010. Long-term effects of fragmentation and fragment properties on bird species richness in Hawaiian forests. Biological Conservation 143:280–288.

Fletcher, R. J., Jr. 2005. Multiple edge effects and their implications in fragmented landscapes. Journal of Animal Ecology 74:342–352.

Gardner, T. A., J. Barlow, R. L. Chazdon, R. M. Ewers, C. A. Harvey, C. A. Peres, and N. S. Sodhi. 2009. Prospects for tropical forest biodiversity in a human-modified world. Ecology Letters 12:561–582.

Giardina, C. P., R. L. Sanford, Jr., and I. C. Døckersmith. 2000. Changes in soil phosphorus and nitrogen during slash-and-burn clearing of a dry tropical forest. Soil Science Society of America Journal 64:399–405.

Harper, K. A., S. E. Macdonald, P. J. Burton, J. Chen, K. D. Brosofske, S. C. Saunders, E. Euskirchen, D. A. Roberts, M. S. Jaiteh, and P. Esseen. 2005. Edge influence on forest structure and composition in fragmented landscapes. Conservation Biology 19:768–782.

Harper, K. A., L. Mascarúa-López, S. E. Macdonald, and P. Drapeau. 2007. Interaction of edge influence from multiple edges: examples from narrow corridors. Plant Ecology 192:71–84.

Herbert, D. A., and J. H. Fownes. 1997. Effects of leaf aggregation in a broad-leaf canopy on estimates of leaf area index by the gap-fraction method. Forest Ecology and Management 97:277–282.

Higgs, A. J., and M. B. Usher. 1980. Should nature reserves be large or small? Nature 285:568–569.

Isenburg, M. 2013. LAStools: efficient tools for LiDAR processing. Version 20130506. Rapid Lasso, Gilching, Germany.

Kapos, V., E. Wandelli, J. L. C. Camargo, and G. Ganade. 1997. Edge-related changes in environment and plant responses due to forest fragmentation in central Amazonia. Pages 33–44 *in* W. F. Laurance and R. O. Bierregaard, Jr., editors. Tropical forest remnants: ecology, management, and conservation of fragmented communities. University of Chicago Press, Chicago, Illinois, USA.

Kobe, R. K. 1999. Light gradient partitioning among tropical tree species through differential seedling mortality and growth. Ecology 80:187–201.

Krauss, J., et al. 2010. Habitat fragmentation causes immediate and time-delayed biodiversity loss at different trophic levels. Ecology Letters 13:597–605.

Laurance, W. F. 2002. Hyperdynamism in fragmented habitats. Journal of Vegetation Science 13:595–602.

Laurance, W. F., J. L. C. Camargo, R. C. C. Luizão, S. G. W. Laurance, S. L. Pimm, E. M. Bruna, P. C. Stouffer, G. Bruce

Williamson, J. Benítez-Malvido, and H. L. Vasconcelos. 2011. The fate of Amazonian forest fragments: a 32-year investigation. Biological Conservation 144:56–67.

Laurance, W. F., T. E. Lovejoy, H. L. Vasconcelos, E. M. Bruna, R. K. Didham, P. C. Stouffer, C. Gascon, R. O. Bierregaard, Jr., S. G. W. Laurance, and E. Sampaio. 2002. Ecosystem decay of Amazonian forest fragments: a 22-year investigation. Conservation Biology 16:605–618.

Laurance, W. F., and E. Yensen. 1991. Predicting the impacts of edge effects in fragmented habitats. Biological Conservation 55:77–92.

Lieberman, M., D. Lieberman, R. Peralta, and G. S. Hartshorn. 1995. Canopy closure and the distribution of tropical forest tree species at La Selva, Costa Rica. Journal of Tropical Ecology 11:161–177.

Lindenmayer, D. B., and J. Fischer. 2006. Managing landscape pattern to mitigate the decline on species and assemblages. Pages 197–212 *in* D. B. Lindenmayer and J. Fischer, editors. Habitat fragmentation and landscape change: an ecological and conservation synthesis. Island Press, Washington, D.C., USA.

Lockwood, J. P., and P. W. Lipman. 1987. Holocene eruptive history of Mauna Loa volcano. Pages 509–535 *in* R. W. Decker, T. L. Wright, and P. H. Stauffer, editors. Professional Paper 1350: Volcanism in Hawaii. United States Geological Survey, Denver, Colorado, USA.

Matlack, G. R. 1993. Microenvironment variation within and among forest edge sites in the eastern United States. Biological Conservation 66:185–194.

McGarigal, K., and S. A. Cushman. 2002. Comparative evaluation of experimental approaches to the study of habitat fragmentation effects. Ecological Applications 12:335–345.

Milne, B. T. 1988. Measuring the fractal geometry of landscapes. Applied Mathematics and Computation 27:67–79.

Montgomery, R. A., and R. L. Chazdon. 2001. Forest structure, canopy architecture, and light transmittance in tropical wet forests. Ecology 82:2707–2718.

Murcia, C. 1995. Edge effects in fragmented forests: implications for conservation. Trends in Ecology and Evolution 10:58–62.

Nicotra, A. B., R. L. Chazdon, and S. V. B. Iriarte. 1999. Spatial heterogeneity of light and woody seedling regeneration in tropical wet forests. Ecology 80:1908–1926.

Patton, D. R. 1975. A diversity index for quantifying habitat "edge". Wildlife Society Bulletin 3:171–173.

Prescott, C. E. 2002. The influence of the forest canopy on nutrient cycling. Tree physiology 22:1193–1200.

Pütz, S., J. Groeneveld, L. F. Alves, J. P. Metzger, and A. Huth. 2011. Fragmentation drives tropical forest fragments to early successional states: a modelling study for Brazilian Atlantic forests. Ecological Modelling 222:1986–1997.

R Development Core Team. 2012. R: a language and environment for statistical computing. Version 2.14.2. R Foundation for Statistical Computing, Vienna, Austria. http://www.r-project.org

Ribeiro, M. C., J. P. Metzger, A. C. Martensen, F. J. Ponzoni, and M. M. Hirota. 2009. The Brazilian Atlantic Forest: how much is left, and how is the remaining forest distributed? Implications for conservation. Biological Conservation 142:1141–1153.

Riitters, K. H., R. V. O. Neill, C. T. Hunsaker, J. D. Wickham, D. H. Yankee, S. P. Timmins, K. B. Jones, and B. L. Jackson. 1995. A factor analysis of landscape pattern and structure metrics. Landscape Ecology 10:23–39.

Riitters, K., J. Wickham, R. O'Neill, B. Jones, and E. Smith. 2000. Global-scale patterns of forest fragmentation. Conservation Ecology 4:18.

Running, S. W., and S. T. Gower. 1991. FOREST-BGC, a general model of forest ecosystem processes for regional applications II: dynamic carbon allocation and nitrogen budgets. Tree Physiology 9:147–160.

Russell, G., P. G. Jarvis, and J. L. Monteith. 1989. Absorption of radiation by canopies and stand growth. Pages 21–39 *in* G. Russell, B. Marshall, and P. G. Jarvis, editors. Plant canopies: their growth, form, and function. Cambridge University Press, Cambridge, UK.

Saunders, D. A., R. J. Hobbs, and C. R. Margules. 1991. Biological consequences of ecosystem fragmentation: a review. Conservation Biology 5:18–32.

Suzuki, S. N., H. Tomimatsu, Y. Oishi, and Y. Konno. 2013. Edge-related changes in tree communities in the understory of mesic temperate forest fragments of northern Japan. Ecological Research 28:117–124.

Thébaud, C., and D. Strasberg. 1997. Plant dispersal in fragmented landscapes: a field study of woody colonization in rainforest remnants of the Mascarene Archipelago. Pages 321–332 *in* W. F. Laurance and R. O. Bierregaard, Jr., editors. Tropical forest remnants: ecology, management and conservation of fragmented communities. University of Chicago Press, Chicago, Illinois, USA.

Vaughn, N. R., G. P. Asner, and C. P. Giardina. 2013. Polar grid fraction as an estimator of forest canopy structure using airborne LiDAR. International Journal of Remote Sensing 34:7464–7473.

Weiskittel, A. R., D. W. Hann, J. A. Kershaw, and J. K. Vanclay. 2011. Process-based models. Pages 227–252 *in* Forest Growth and Yield Modeling. First edition. Wiley-Blackwell, Chichester, UK.

Supplemental Material

Supplement 1

A vector file of polygon fragment boundaries used in this study in KML format (*Ecological Archives* A024-197-S1).

Supplement 2

A listing containing code to perform the minimum span computation in C syntax (*Ecological Archives* A024-197-S2).